ChemPubSoc Europe

DOI: 10.1002/cphc.201900839

CHEMPHYSCHEM Articles

Opposing Electronic and Nuclear Quantum Effects on Hydrogen Bonds in H_2O and D_2O

Timothy Clark,*[a] Julian Heske,[b] and Thomas D. Kühne*[b]

The effect of extending the O–H bond length(s) in water on the hydrogen-bonding strength has been investigated using static ab initio molecular orbital calculations. The "polar flattening" effect that causes a slight σ-hole to form on hydrogen atoms is strengthened when the bond is stretched, so that the σ-hole becomes more positive and hydrogen bonding stronger. In opposition to this electronic effect, path-integral ab initio molecular-dynamics simulations show that the nuclear quantum effect weakens the hydrogen bond in the water dimer. Thus, static electronic effects strengthen the hydrogen bond in H_2O relative to D_2O, whereas nuclear quantum effects weaken it. These quantum fluctuations are stronger for the water dimer than in bulk water.

1. Introduction

In the grand scheme of things, hydrogen bonding punches well above its weight.[1] The unusual properties of water are largely due to hydrogen bonding,[2] so that evolution has adapted nature to fit the hydrogen-bonding properties of normal water, making D_2O quite toxic,[3] whereby both kinetic effects and changed hydrogen-bonding properties are likely to be important. D_2O is thought to form weaker hydrogen bonds than H_2O.[4] This hypothesis is supported by its larger molar volume (30.07 $Å^3 mol^{-1}$) at maximum density compared with H_2O (29.91 $Å^3 mol^{-1}$)[5] despite its smaller dimensions at room temperature[6] and by the fact that the experimental hydrogen-bond distance in D_2O is 4% longer than in H_2O.[7] In contrast, the heat of vaporization and cohesive energy density of D_2O (10.85 kcal mol^{-1} and 565 cal $mol^{-1} cm^{-1}$, respectively) are higher than those of H_2O (10.52 kcal mol^{-1} and 549 cal $mol^{-1} cm^{-1}$).[2,8] However, these numbers are affected by the higher average number of hydrogen bonds per molecule in D_2O (3.76) than in H_2O (3.62).[7] If this correction is applied naively to the heat of vaporization, D_2O has an approximately 1% lower energy per hydrogen bond than H_2O.

D_2O is known to stabilize proteins (i.e. increase the temperature at which they denature), make them more compact and less flexible than in H_2O[9–11] and enhance aggregation,[9,12] suggesting that it shifts the equilibrium between inter-residue hydrogen bonds and competing ones to the solvent in favor of the former. D_2O behaves in many respects quite differently to H_2O. For instance, cyclodextrins are approximately 40% less soluble in D_2O than in H_2O,[13] polar amino acids are more soluble in D_2O and proline in H_2O.[14] pKAs are also significantly different in D_2O than in H_2O.[15] These effects have been rationalized in a variety of ways, none of which seems to be able to explain everything, although the idea that the cohesive energy density of D_2O strengthens hydrophobic interactions is widespread.[8] Ten years ago, in an extensive review of quantum simulations of water, Peasani and Voth[9] concluded that "*From a theoretical point of view, very little is known about the effects of D_2O on the properties of biomolecules*".

Traditionally, rationalizations of D_2O's remarkably different properties to H_2O have centered on vibrational or quantum mechanical effects in the nuclear dynamics. These differ strongly between the two isotopes because deuterium is twice as heavy as hydrogen. Car-Parrinello density-functional theory (DFT) path-integral molecular-dynamics simulations have been used to simulate water and D_2O[16] and give far better agreement with experiment than classical simulations. These simulations include both electronic and nuclear quantum effects (NQE). However, the DFT technique employed does not reproduce dispersion, which is likely to be a small but significant part of hydrogen bonding.[17] The traditional "organic" view is simply that deuterium is more electronegative than hydrogen.[18] This view is hard to justify rigorously but does rationalize many experimental observations. We now report high-level static *ab initio* molecular orbital calculations and *ab initio* path-integral molecular-dynamics (AI-PIMD) simulations. They demonstrate that hydrogen bonding in the water dimer depends significantly on the O–H bond lengths, so that some of the observed difference between H_2O and D_2O can be attributed to an electronic quantum mechanical effect, which, however, is opposed by NQE effects.

[a] *Prof. Dr. T. Clark*
Computer-Chemie-Centrum, Department Chemie und Pharmazie, Friedrich-Alexander-Universität Erlangen-Nürnberg, Nägelsbachstr. 25, 91052 Erlangen, Germany
E-mail: tim.clark@fau.de
[b] *J. Heske, Prof. Dr. T. D. Kühne*
Chair of Theoretical Chemistry, Dynamics of Condensed Matter, Department of Chemistry, University of Paderborn, Warburger Str. 100, 33098 Paderborn, Germany
E-mail: tdkuehne@mail.upb.de

Supporting information for this article is available on the WWW under https://doi.org/10.1002/cphc.201900839

2. Methods

The C_s water dimer structure shown below was used for all static calculations. It contains three types of hydrogen atom; the donor hydrogen H_D, the remote hydrogen on the donor water molecule H_R, and the two equivalent hydrogen atoms on the acceptor water H_A.

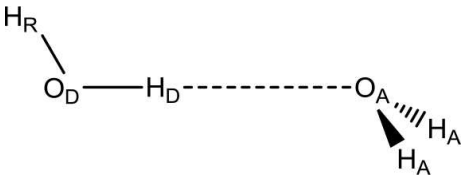

Geometry optimizations were performed at the MP2[19]/aug-cc-pVTZ[20] level without counterpoise corrections, which amount to 0.17 kcal mol^{-1} at this level. Calculations were also performed with a counterpoise correction but lead to the same conclusions as those without. Details are provided in the Supporting Information. Full geometry optimization within C_s symmetry was confirmed to give a minimum-energy structure by calculating the normal vibrations within the harmonic approximation. Additionally, four series of calculations were performed in which the O_D–H_D and O_D–H_R bond lengths, both bond lengths to O_D and both bond lengths to OA were constrained to values of 0.97, 0.98, 0.99 and 1.00 Å. All other geometrical parameters were optimized fully within C_s symmetry. Single-point CCSD(T)[21,22]/aug-cc-pVTZ calculations were performed on the optimized geometries in order to obtain refined Born-Oppenheimer hydrogen-bonding energies. Parallel calculations at the same levels were performed for the distorted water monomers in order to obtain the hydrogen-bonding energies ΔE_{HB}, which are defined as

$$\Delta E_{HB} = E^{Tot}_{Dimer,constrained} - E^{Tot}_{H2O,opt} - E^{Tot}_{H2O,constrained} \quad (1)$$

where $E^{Tot}_{dimer,constrained}$ is the CCSD(T)/aug-cc-pVTZ total energy of the constrained dimer, $E^{Tot}_{H2O,constrained}$ that of a monomer subject to exactly the same geometrical constraints as for the dimer and $\Delta E_{H2O,opt}$ that of the fully optimized monomer. Thus, ΔE_{HB} represents the hydrogen-bonding energy of the distorted monomer with a second unconstrained water molecule. All static calculations used Gaussian09.[23]

We have also performed AI-PIMD simulations[24,25] in order to assess the impact of finite-temperature and NQE on the structure of the individual water molecules of the water dimer and the bulk. The second-generation Car-Parrinello-based quantum ring-polymer contraction method of Kühne and coworkers was used.[26,27] This approach not only permits substantial acceleration compared to conventional Car-Parrinello molecular dynamics simulations,[27] but also includes NQE explicitly at no additional computational cost.[28] Specifically, the interatomic forces were computed at the DFT/TZV2P level of theory using the CP2 K Quickstep code[29] with the TPSS exchange and correlation functional[30,31] in conjunction with Grimme's D3 dispersion correction,[32] whereas the force-matched fm-TIP4P/F-TPSS-D3 water was used as the computationally inexpensive auxiliary potential.[33] The equations of motion for the AI-PIMD at 50 K using 128 ring-polymer beads were integrated using the i-Pi interface.[34]

Note that, for water clusters, even rigorously including nuclear quantum effects, path-integral molecular dynamics simulations at the MP2 and even CCSD levels of theory are feasible.[35] However, in this study we investigate the impact of NQE and finite temperature effects consistently for isolated molecules and bulk water. For the latter, no more accurate treatment than the DFT level of theory used is feasible. However, the TPSS-D3 exchange and correlation functional used systematically outperforms the popular PBE-D3 functional and gives a mean absolute deviation of less than 5 kcal mol^{-1} with respect to CCSD and MP2 reference calculations extrapolated to the complete basis set limit for the WATER27 benchmark.[36]

3. Results

Figure 1 shows the hydrogen-bond energies obtained in the static calculations as a function of the constrained O–H bond length.

Lengthening the O–H bonds results in increased ΔE_{HB} for the O_D–H_D and O_A–H_A bonds and the opposite for the O_D–H_R bond. However, lengthening both bonds to O_D results in an increase in ΔE_{HB} that is almost as large as that found for O_D–H_D alone. The largest effect is found when O_D–H_D is lengthened. The vertical dashed lines in Figure 1 indicate the bond lengths in H_2O (0.972 Å and 0.985 Å in the gas[6] and liquid[37] phases, respectively) and D_2O (0.969 and 0.990 Å). They indicate that the hydrogen bond in an H_2O dimer should be approximately 1.0% more stable than in the corresponding D_2O dimer, exactly as the O–H bond in liquid H_2O is found to be 1.0% longer than its equivalent in D_2O.

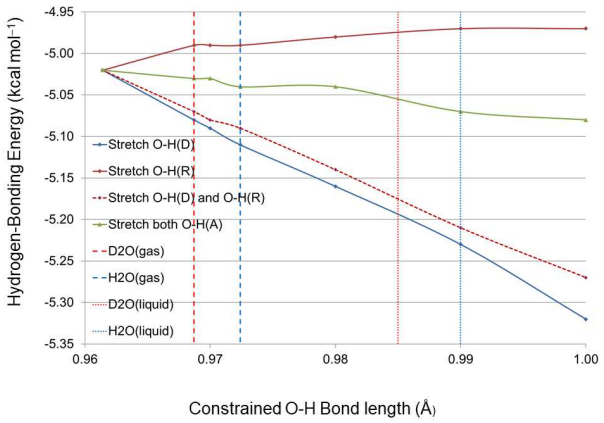

Figure 1. Dependence of the calculated (CCSD(T)/CBS) Born-Oppenheimer hydrogen-bonding energies (as defined in Equation (1)) on the length of the constrained OH-bond(s). The vertical dashed lines indicate the experimental bond lengths observed for D_2O (red) and H_2O (blue). The gas-phase and liquid values are taken from references [6] and [7], respectively.

As can be seen in Table S2, the AI-PIMD simulations showed that both intermolecular distances are increased due to NQE (up to 4% for the $H_D\cdots O_A$ distance), which is consistent with previous PIMD simulations and experimental measurements of liquid water.[7,33] Interestingly, however, the intramolecular O–H bonds are, on the one hand, shortened by up to 5% (O_D–HR) by NQE, whereas in bulk water they are slightly elongated.[33] Moreover, the intramolecular angles are increased by as much as 1% (H_R–O_D–H_D), which again contrasts with the bulk, where the intramolecular angles are slightly decreased due to NQE.[33] As expected, the impact of NQE is particularly pronounced for H_2O, followed by HDO and D_2O.

4. Discussion

We have previously pointed out that polarization of the O–H bond in hydrogen-bond donors has a large effect on the strength of hydrogen bonding.[38] This is because of the polar flattening effect observed for A–H bonds (A is an electronegative element).[39,40]

Such bonds are easily polarized because the electron density assignable to the hydrogen atom is shifted into the A–H bond and can be moved towards or away from the hydrogen atom by applied fields.[41] A similar effect is responsible for the data reported above, as shown schematically in Figure 2.

This can be seen in the molecular electrostatic potential plotted[42] at the standard 0.001 electron $Bohr^{-3}$ isodensity surface[43] of water in which one bond has been extended to 0.99 Å, as shown in Figure 3.

In this case, the σ-hole on the right-hand hydrogen (the one with the longer bond) is more pronounced than that on the other. This effect amounts to a perturbation of approximately 2% (the most positive MP2/aug-cc-pVTZ MEP at the isodensity surface on the left and right hydrogen atoms is +44.0 and +45.0 kcal mol^{-1}, respectively) and is directly related to ΔE_{HB}.[44]

The hydrogen bond ($H_D\cdots O_A$) distance also increases as the O–H bonds are stretched, as shown in Figure 4.

The total Born-Oppenheimer shortening of the ($H_D\cdots O_A$) hydrogen bond as the constrained O_D–H_D bond length increases from 0.96 to 1.00 Å amounts to 1.7%. This is less than half of the 4% observed experimentally,[7] which shows that some of the shortening is a purely electronic effect, not only one of NQE.

As pointed out above, the explicit inclusion of NQE entails an increase in the intermolecular distance, which is a consequence of intermolecular quantum fluctuations that are known to weaken hydrogen bonds.[45] Then again, the intramolecular distance is reduced due to NQE, while, at the same time, the intramolecular angle increases, in contrast to the bulk. Together, this immediately suggests an NQE-induced reduction of the molecular dipole moment, as is also seen directly in the present CCSD(T)/aug-cc-pVTZ calculations.

These intramolecular zero-point fluctuations in the anharmonic O–H stretching coordinate are most likely a consequence that, for the low-temperature water dimer, the intramolecular

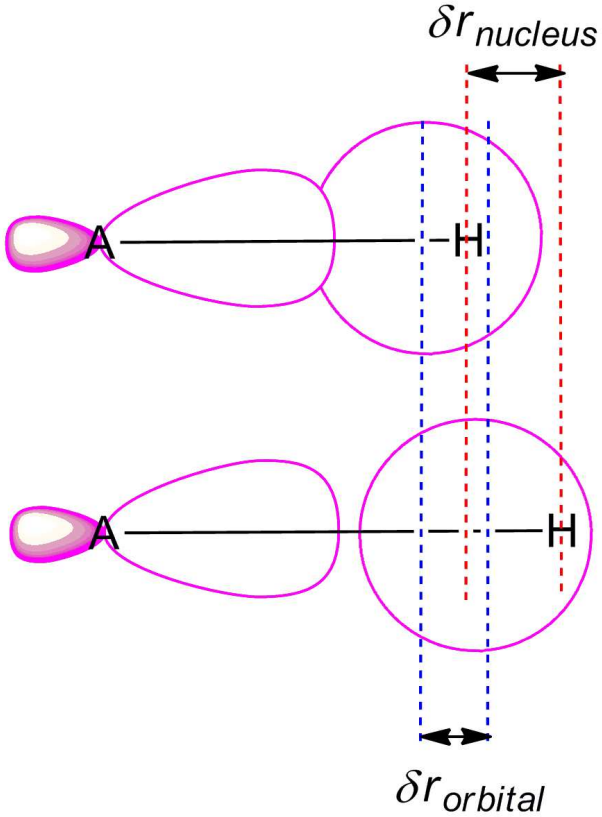

Figure 2. Schematic diagram of the effect of lengthening an A–H bond. When the distance between the nuclei is increased by $\delta r_{nucleus}$, the center of the electron density assignable to the hydrogen 1 s-orbital moves by $\delta r_{orbital}$. This distance is smaller than $\delta r_{nucleus}$ because the attraction due to the single nuclear charge of the hydrogen is unable to compensate for the loss of bonding overlap in the A–H bond as the bond is extended.

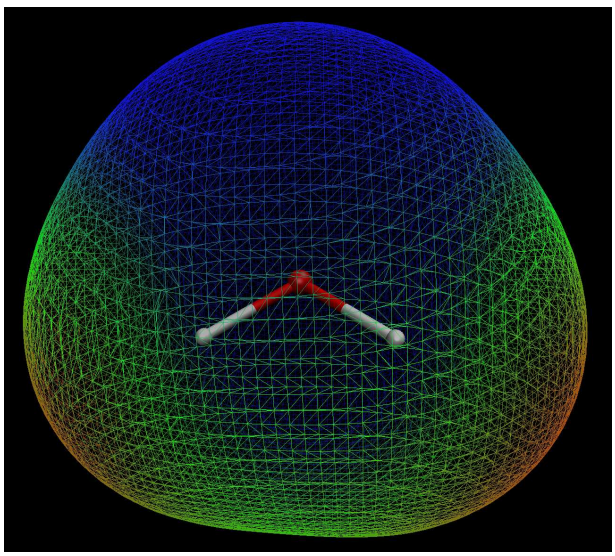

Figure 3. The molecular electrostatic potential at the 0.001 a.u. isodensity surface calculated using the MP2/aug-cc-pVTZ electron density for a water molecule in which the right-hand O–H bond has been fixed at 1.00 Å and both other geometrical degrees of freedom optimized. The left-hand O–H bond length is 0.960 Å. The color scale ranges from −44 (blue) to +50 (red) kcal mol^{-1}.

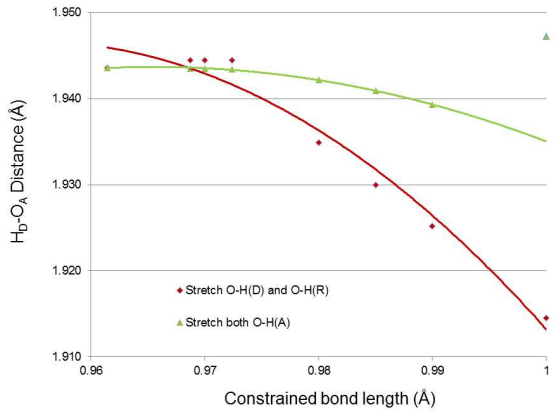

Figure 4. The dependence of the hydrogen-bond (H_D···O_A) length on that of the constrained O–H bonds. A discontinuity occurs if both O–H_A bonds are stretched to 1 Å.

potential is rather hard. In any case, a smaller molecular dipole moment entails even weaker intermolecular interactions between the two water molecules.

In other words, contrary to bulk water at ambient conditions, where a competition between inter- and intramolecular quantum fluctuations has been proposed,[46] we find that for the low-temperature water dimer NQE are cooperative. This is to say that the well-known weakening of hydrogen bonds in liquid water due to NQE is even more pronounced in the low-temperature water dimer, which explains the rather large increase in the intermolecular distance. Because NQE are generally larger in H_2O than in D_2O hydrogen bonds, the former are weakened most by quantum fluctuations. This leads to the surprising conclusion the static-electronically weaker hydrogen-bond in D_2O becomes stronger when NQE are taken into account, which is consistent with AI-PIMD simulations of others.[28] This effect is, however, weaker in bulk water than in the isolated water dimer.

5. Conclusions

The above calculations suggest that the difference in hydrogen-bond strength between D_2O and H_2O exists even at absolute zero and is caused by changes in the molecular wavefunction that result from the lengthening of the O–H bonds by zero-point vibrations, especially in the very anisotropic O_D–H_D bond. Further vibrational effects are likely as the temperature increases, but there remains an underlying difference in the inherent hydrogen-bonding strength of the two molecules. These conclusions are reflected in the experimental observations that "deuterium is more electronegative than protium"[18] and in the idea[37] that the dipole moment of O–H bonds is larger than that of inherently shorter O–D bonds. The observed electronic effect is, however, more subtle and is better described by Figure 2. H_2O is both a better hydrogen-bond donor and acceptor than D_2O, although the former effect is larger, as shown in Figure 1. Atomistic force fields designed to reproduce differences between H_2O and D_2O should give slightly (approximately 1%) weaker hydrogen bonds for deuterium than hydrogen in addition to being polarizable. The inclusion of NQE, however, causes that the initially stronger hydrogen bond of H_2O eventually becomes weaker due to the quantum fluctuation induced cooperative weakening, which is particular pronounced for H and the present low-temperature water dimer.

Acknowledgements

This work was supported by the Deutsche Forschungsgemeinschaft as part of the Excellence Cluster "Engineering of Advanced Materials" and by the European Research Council (ERC) under the European Union's Horizon 2020 research and innovation programme (Grant Agreement No.: 716142). TC thanks Jon Essex, Frank Beierlein, Peter Politzer and Jane Murray for discussions that led to this work. JH and TDK acknowledge the generous allocation of computing time on OCuLUS and the FPGA-based supercomputed NOCTUA by the Paderborn Center for Parallel Computing (PC²).

Conflict of Interest

The authors declare no conflict of interest.

Keywords: ab initio calculations · bond theory · hydrogen bonds · isotope effects · solvent effects

[1] G. A. Jeffrey, W. Saenger, *Hydrogen bonding in biological structures*, Springer Verlag, New York **1991**.
[2] D. Eisenberg, W. Kauzmann, *The structure and properties of water*, Clarendon press, Oxford **2005**.
[3] D. J. Kushner, A. Baker, T. G. Dunstall, *Can. J. Physiol. Pharmacol.* **1999**, *77*, 79–88.
[4] H. Schott, *J. Macromol. Sci. Phys.* **1988**, *B27*, 119–123.
[5] F. Franks, *Water: A matrix of life*, 2nd Edition, Royal Society of Chemistry, Cambridge **2000**.
[6] R. L. Cook, F. C. Deluciaand, P. Helminge, *J. Mol. Spectrosc.* **1974**, *53*, 62–76.
[7] A. K. Soper, C. J. Benmore, *Phys. Rev. Lett.* **2008**, *101*, 065502.
[8] G. Graziano, *J. Chem. Phys.* **2004**, *121*, 1878–1882.
[9] F. Paesani, G. V. Voth, *J. Chem. Phys.* **2009**, *113*, 5702–5719 and references therein.
[10] M. J. Parker, A. R. Clarke, *Biochem.* **1997**, *36*, 5786–5794.
[11] P. Cioni, G. B. Strambini, *Biophys. J.* **2002**, *82*, 3246–3253.
[12] D. Panda, G. Chakrabarti, J. Hudson, K. Pigg, H. P. Miller, L. Wilson, R. H. Himes, *Biochem.* **2000**, *39*, 5075–5081.
[13] M. V. C. Cardoso, L. V. C. Carvalho, E. Sabadini, *Carbohydr. Res.* **2012**, *353*, 57–61.
[14] M. Jelinska-Kazimierczuk, J. Szydlowski, *J. Solution Chem.* **1996**, *25*, 1175–1184.
[15] R. A. Robinson, M. Paabo, R. G. Bates, *J. Res. Natl. Bur. Stand. Sect. A* **1969**, *73 A*, 299–308.
[16] B. Chen, I. Ivanov, M. L. Klein, M. Parrinello, *Phys. Rev. Lett.* **2003**, *91*, 215503.
[17] M. M. Szcześniak, Z. Latajka, S. Scheiner, *J. Mol. Struct.*, **1986**, *135*, 179–188.
[18] A. Streitwieser, H. S. Klein, *J. Am. Chem. Soc.* **1963**, *85*, 2759–2763.

[19] M. Head-Gordon, J. A. Pople, M. J. Frisch, *Chem. Phys. Lett.* **1988**, *153*, 503–506.
[20] T. H. Dunning Jr, *J. Chem. Phys.* **1989**, *90*, 1007–1023.
[21] G. E. Scuseria, C. L. Janssen, H. F. Schaefer, *J. Chem. Phys.* **1988**, *89*, 7382–7387.
[22] J. A. Pople, M. Head-Gordon, K. Raghavachari, *J. Chem. Phys.* **1987**, *87*, 5968–5975.
[23] M. J. Frisch, G. W. Trucks, H. B. Schlegel, G. E. Scuseria, M. A. Robb, J. R. Cheeseman, G. Scalmani, V. Barone, B. Mennucci, G. A. Petersson, H. Nakatsuji, M. Caricato, X. Li, H. P. Hratchian, A. F. Izmaylov, J. Bloino, G. Zheng, J. L. Sonnenberg, M. Hada, M. Ehara, K. Toyota, R. Fukuda, J. Hasegawa, M. Ishida, T. Nakajima, Y. Honda, O. Kitao, H. Nakai, T. Vreven, J. J. A. Montgomery, J. E. Peralta, F. Ogliaro, M. Bearpark, J. J. Heyd, E. Brothers, K. N. Kudin, V. N. Staroverov, R. Kobayashi, J. Normand, K. Raghavachari, A. Rendell, J. C. Burant, S. S. Iyengar, J. Tomasi, M. Cossi, N. Rega, J. M. Millam, M. Klene, J. E. Knox, J. B. Cross, V. Bakken, C. Adamo, J. Jaramillo, R. Gomperts, R. E. Stratmann, O. Yazyev, A. J. Austin, R. Cammi, C. Pomelli, J. W. Ochterski, R. L. Martin, K. Morokuma, V. G. Zakrzewski, G. A. Voth, P. Salvador, J. J. Dannenberg, S. Dapprich, A. D. Daniels, Ö. Farkas, J. B. Foresman, J. V. Ortiz, J. Cioslowski, D. J. Fox, Gaussian 09, Revision A.02, Gaussian, Inc.: Wallingford CT, **2009**.
[24] D. Marx, M. Parrinello, *J. Chem. Phys.* **1996**, *104*, 4077–4082.
[25] M. E. Tuckerman, D. Marx, M. L. Klein, M. Parrinello, *J. Chem. Phys.* **1996**, *104*, 5579–5588.
[26] T. D. Kühne, M. Krack, F. R. Mohamed, M. Parrinello, *Phys. Rev. Lett.* **2007**, *98*, 066401.
[27] C. John, T. Spura, S. Habershon, T. D. Kühne, *Phys. Rev. E* **2016**, *93*, 043305.
[28] V. Kapil, J. VandeVondele, M. Ceriotti, *J. Chem. Phys.* **2016**, *144*, 054111.
[29] R. O. Jones, O. Gunnarsson, *Rev. Mod. Phys.* **1989**, *61*, 689–748.
[30] J. Van de Vondele, M. Krack, F. Mohamed, M. Parrinello, T. Chassaing, J. Hutter, *Comput. Phys. Commun.* **2005**, *167*, 103–128.
[31] J. Tao, J. P. Perdew, V. N. Staroverov, G. E. Scuseria, *Phys. Rev. Lett.* **2003**, *91*, 146401.
[32] S. Grimme, J. Antony, S. Ehrlich, H Krieg, *J. Chem. Phys.* **2010**, *132*, 154104.
[33] T. Spura, C. John, S. Habershon, T. D. Kühne, *Mol. Phys.* **2015**, *113*, 808.
[34] V. Kapil, M. Rossi, O. Marsalek, R. Petragia, Y. Litman, T. Spura, B. Cheng, A. Cuzzocrea, R. H. Meißner, D. M. Wolkins, B. A. Helcfrecht, P. Juda, S. P. Bienvenue, W. Fang, J. Kessler, I. Poltavsky, S. Vandenbrande, J. Wierme, C. Corminboeuf, T. D. Kühne, D. E. Manolopoulos, T. E. Markland, J. O. Richardson, A. Tkatchenko, G. A. Tribello, V. Van Speyrbroeck, M. Cerlotti, *Comput. Phys. Commun.* **2019**, *236*, 214–223.
[35] T. Spura, H. Elgabarty, T. D. Kühne, *Phys. Chem. Chem. Phys.* **2015**, *17*, 14355.
[36] L. Goerigk, S. Grimme, *Phys. Chem. Chem. Phys.* **2011**, *13*, 6670–6688.
[37] A. Zeidler, P. S. Salmon, H. E. Fischer, J. C. Neuefeind, J. M. Simonson, T. E. Markland, *J. Phys. Condens. Matter* **2012**, *24*, 284126.
[38] M. Hennemann, J. S. Murray, P. Politzer, K. E. Riley, T. Clark, *J. Mol. Model.* **2012**, *18*, 2461–2469.
[39] O. Ermer, S. Lifson, *J. Am. Chem. Soc.* **1973**, *95*, 4121–4132.
[40] U. Burkert, N. L. Allinger, *Molecular Mechanics, ACS Monograph 177*, American Chemical Society: Washington, DC, **1972**.
[41] L. Fielder, J. Gao, D. G. Truhlar, *J. Chem. Theory Comput.* **2011**, *7*, 852–856.
[42] W. Humphrey, A. Dalke, K. Schulten, *J. Mol. Graphics* **1996**, *14*, 33–38.
[43] R. F. W. Bader, M. T. Carroll, J. R. Cheeseman, C. Chang, *J. Am. Chem. Soc.* **1987**, *109*, 7968–7679.
[44] K. E. Riley, J. S. Murray, M. C. Concha, P. Hobza, P. Politzer, *J. Chem. Theory Comput.* **2009**, *5*, 155–163.
[45] S. Habershon, T. E. Markland, D. E. Manolopoulos, *J. Chem. Phys.* **2009**, *131*, 024501.
[46] X.-Z. Li, B. Walker, A. Michaelides, *Proc. Natl. Acad. Sci. USA* **2011**, *108*, 6369–6373.

Manuscript received: August 23, 2019
Accepted manuscript online: August 26, 2019
Version of record online: September 10, 2019